Magnetic Resonance Imaging 57 (2019) 28–33

Contents lists available at ScienceDirect

Magnetic Resonance Imaging

journal homepage: www.elsevier.com/locate/mri

Original contribution

A study of neurite orientation dispersion and density imaging in ischemic stroke

Zhenxiong Wang, Shun Zhang, Chengxia Liu, Yihao Yao, Jingjing Shi, Ju Zhang, Yuanyuan Qin, Wenzhen Zhu*

Department of Radiology, Tongji Hospital, Tongji Medical College, Huazhong University of Science and Technology, No. 1095 Jiefang Avenue, Wuhan 430030, China

ARTICLE INFO

Keywords:
Neurite orientation dispersion and density imaging
Diffusion magnetic resonance imaging
Stroke

ABSTRACT

Objectives: To demonstrate the feasibility of the neurite orientation dispersion and density imaging (NODDI) technique in characterizing the microstructural changes in brain tissues during ischemic stroke and to compare its sensitivity with diffusion tensor imaging (DTI) and diffusion kurtosis imaging (DKI).

Methods: Seventy-one patients with hyperacute/acute/subacute ischemic stroke were enrolled in the study. A multishell diffusion magnetic resonance imaging (dMRI) protocol was performed for each subject. Diffusion data were analyzed using the NODDI and diffusional kurtosis estimator toolboxes. Then, NODDI metrics between the lesions and the contralateral tissues were compared to evaluate their values in ischemic stroke. NODDI metrics among different stroke periods and the correlations between NODDI and the duration since stroke onset were analyzed as well. To compare the NODDI's sensitivity with established diffusion techniques, paired *t*-tests were performed to determine the absolute percentage changes of diffusion metrics between NODDI and DTI/DKI.

Results: Compared with the contralateral tissues, lesions showed significantly increased values of intracellular volume fraction (V_{ic}) and orientation dispersion index (ODI) and decreased values of isotropic volume fraction (V_{iso}). ODI value was significantly different among three periods and showed fair to good positive correlation with the duration since stroke onset ($R = 0.450$). NODDI metrics showed significantly larger absolute percentage changes than that of DTI and DKI ($P < 0.05$, respectively).

Conclusion: NODDI allowed efficient evaluation of microstructural changes in brain tissues during ischemic stroke and showed increased sensitivity compared with DTI and DKI. The possible biophysical mechanisms underlying ischemia could be further elucidated using this advanced diffusion technique.

1. Introduction

Stroke is one of the most important causes of death and disability in humans, resulting in tremendous social and economic burden [1]. Ischemia is the most important factor in stroke. Thus, accurate assessment of the pathomechanism of ischemic stroke is critical for the diagnosis, treatment, and prognosis of patients.

Nowadays, diffusion magnetic resonance imaging (dMRI) is widely used in the early assessment of ischemic stroke [2,3]. Diffusion tensor imaging (DTI) is the conventional and commonly used clinical dMRI technique. DTI is based on the Gaussian distribution assumption of diffusion processes, which may not be appropriate to describe the non-Gaussian diffusion processes in biological tissues [4]. As the extension of DTI, diffusion kurtosis imaging (DKI) is a common non-Gaussian diffusion imaging technique that can reflect the complexity of tissue microstructures to some degree. However, both DTI and DKI cannot disentangle the confounding factors such as neurite density and orientation dispersion contribution to microstructural changes [5]. To address these problems, some advanced diffusion techniques have been proposed, such as the ball-and-stick model, q-ball imaging, diffusion spectrum imaging, composite hindered and restricted model of diffusion, neurite orientation dispersion and density imaging (NODDI), and other high-angular-resolution diffusion imaging models or reconstruction methods [6–12]. Notably, the NODDI technique as an advanced

Abbreviations: dMRI, diffusion MRI; DTI, diffusion tensor imaging; DKI, diffusion kurtosis imaging; NODDI, neurite orientation dispersion and density imaging; V_{ic}, intracellular volume fraction; ODI, orientation dispersion index; V_{iso}, isotropic volume fraction; rV_{ic}, relative intracellular volume fraction; rODI, relative orientation dispersion index; rV_{iso}, relative isotropic volume fraction; GM, gray matter; WM, white matter; DKE, diffusion kurtosis estimator; MK, mean kurtosis; FA, fractional anisotropy; MD, mean diffusivity; ROI, region of interest; CSF, cerebrospinal fluid

* Corresponding author.
E-mail address: zhuwenzhen8612@163.com (W. Zhu).

https://doi.org/10.1016/j.mri.2018.10.018
Received 1 June 2018; Received in revised form 25 October 2018; Accepted 27 October 2018

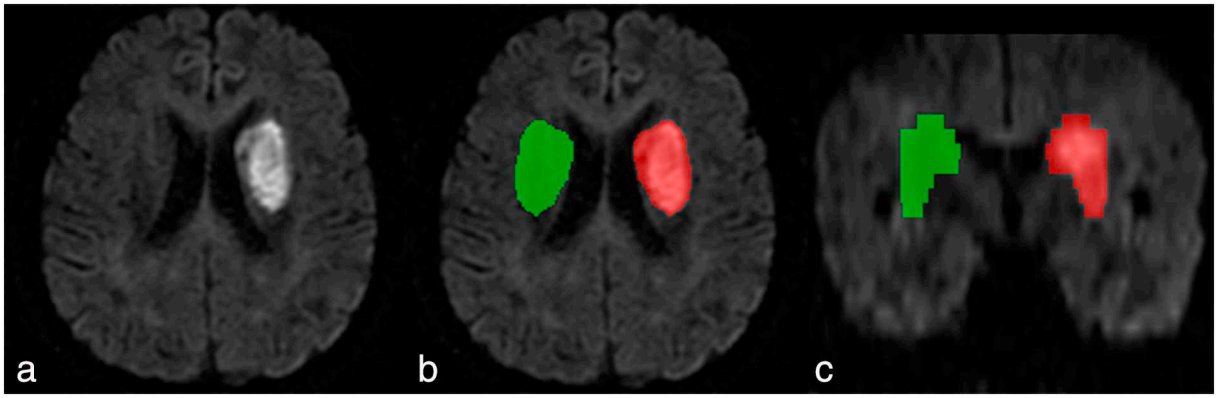

Fig. 1. ROIs encompassing lesion and contralesional tissue. Lesion was hyperintense on diffusion image (a). ROIs on axial slice (b) and coronal slice (c). Red indicates lesion, and green indicates normal tissue. (For interpretation of the references to color in this figure legend, the reader is referred to the web version of this article.)

non-Gaussian diffusion model can quantitatively evaluate specific microstructural changes in terms of neurite density and orientation distribution of axons and dendrites. It has been proven to be a more appropriate model to describe the changes in neurite orientation dispersion and density by several previous studies on both healthy subjects and patients with various neurological disorders, such as multiple sclerosis, depressive disorder, Wilson's disease, and so on [5,10–17].

The aim of this study was to evaluate the feasibility of NODDI for quantitatively detecting the microstructural changes in brain tissues during ischemic stroke and to attempt to determine whether NODDI metrics could be used as specific markers to elucidate possible biophysical mechanisms underlying ischemic stroke.

2. Materials and methods

2.1. Patients

This study was approved by the ethics committee of Tongji Hospital, Wuhan, China. Written informed consent was obtained from each participant before the examination. A total of 102 patients with ischemic stroke (53 men, 18 women, mean age 54.0 years, age range 26–80 years) from February 2013 to August 2014 were enrolled in this study. All patients were diagnosed with ischemic stroke according to their clinical and imaging data. The time intervals between symptom onset and MRI examination for all patients were from 6 h to 2 weeks. Of these patients, 31 were excluded because of motion artifacts (n = 15), hemorrhagic transformation (n = 4), contralateral area lesions (n = 3), and small lesion size (minimal diameter $<$ 0.5 cm, n = 9). In addition, patients with a history of brain neoplasm were also excluded from our study. Thus, 71 cases were included for the following analysis. According to previous studies [18], all patients were divided into three groups based on the time from symptom onset to MRI examination: hyperacute period (0 h–6 h, n = 6), acute period (6 h–3 days, n = 23), and subacute period (3 days–2 weeks, n = 42).

2.2. Image acquisition

All MRI examinations were conducted on a 3 T MRI system using a 32-channel head coil (GE Medical Systems, Discovery MR750, Waukesha, WI, USA). For the diffusion imaging, a multishell protocol was performed along 25 noncollinear directions at 3 b-values (0, 1250, and 2500 s/mm^2). Other acquisition parameters were as follows: TR = 5000 ms, TE = 98.1 ms, slice thickness = 4 mm, FOV = 240 × 240 mm^2, matrix size = 128 × 128, NEX = 1, total scan time = 5 min 45 s.

2.3. Imaging analysis

The DICOM data were first converted to NIFTI format. Then, all diffusion data were preprocessed for eddy current distortion, head motion corrections, and brain extraction using FSL (http://fsl.fmrib.ox.ac.uk). After preprocessing steps, NODDI-related metrics (intracellular volume fraction [V_{ic}], orientation dispersion index [ODI], and isotropic volume fraction [V_{iso}]) were generated using the NODDI Matlab Toolbox (http://www.nitrc.org/projects/noddi_toolbox). The full normalized signal S in NODDI can be written as

$$S = (1 - V_{iso})(V_{ic}S_{ic} + (1 - V_{ic})S_{ec}) + V_{iso}S_{iso}$$

where S_{ic} is the non-Gaussian pattern of the intracellular diffusion signal and S_{ec} is the extracellular normalized signal, which represents the space around the axons and dendrites, including various types of glial cells and somas in gray matter (GM). The diffusion of water molecules is hindered but not restricted by the presence of neurites in this compartment. Thus, it is modeled using an anisotropic Gaussian diffusion process. S_{iso} is the normalized signal of the isotropic Gaussian diffusion compartment. In addition, DKI and DTI metrics were calculated using diffusion kurtosis estimator (DKE) software (http://www.nitric.org/projects/dke). DKI-related metric mean kurtosis (MK) and DTI-related metrics including fractional anisotropy (FA) and mean diffusivity (MD) were generated.

Regions of interest (ROIs) were manually drawn along the areas of ischemia with explicit hyperintensity on the mean of all diffusion images with a b-value of 1250 s/mm^2 using ITK-SNAP [19]. To minimize the partial volume effect on the calculation accuracy, the obscure hyperintensity areas were excluded. In addition, the ROIs with multislice rather than a single slice with the largest lesion region were used to allow us to obtain the mean value of the whole lesion without biased analysis about ischemia. Mirrored ROIs were placed and manually modified to represent contralateral normal brain tissues. Cerebrospinal fluid (CSF) or large vessels were also manually excluded in all ROIs. The same ROIs were then overlaid to all dMRI parametric maps. Examples of ROI placement in lesions and contralateral regions are depicted in Fig. 1. All ROIs were outlined by an experienced neuroradiologist (Z.W., 3 years of experience) and confirmed by another neuroradiologist (S.Z., 6 years of experience).

Averaged values of all pixels within each ROI were extracted for all diffusion parameters. Moreover, the relative NODDI (rNODDI) metrics (relative V_{ic} [rV_{ic}], relative ODI [rODI], and relative V_{iso} [rV_{iso}]) from normal to ischemic areas were computed as L/C to standardize the NODDI metric values and partly eliminate the effect of different brain volumes on the assessment of NODDI metrics. The percentage changes of the different diffusion metrics from normal to ischemic areas were computed as [(L − C) / C] × 100%, as well to evaluate the sensitivity, where L and C denote the mean values of the lesions and contralateral

tissues, respectively.

2.4. Statistical analysis

Statistical analysis was performed using Statistical Product and Service Solutions (SPSS, version 19.0, Chicago, IL) software. To assess the value of NODDI, a paired *t*-test was used to compare the mean NODDI parameters between ischemic lesions and contralateral normal tissues. Then, analysis of variance test was performed to compare NODDI/rNODDI metrics between different stroke periods (hyperacute, acute, and subacute). Furthermore, the correlations between NODDI/rNODDI metrics and the duration since stroke onset were also assessed. Pearson's correlation coefficient was considered to be poor ($0 < R \leq 0.2$), weak ($0.2 < R \leq 0.4$), fair to good ($0.40 < R \leq 0.75$), or excellent ($R > 0.75$). To compare the sensitivity in describing ischemic stroke with previous diffusion techniques, paired *t*-tests were performed on absolute percentage changes of diffusion metrics between NODDI and DTI/DKI. For all statistical analysis procedures, $P < 0.05$ was considered statistically significant.

3. Results

Parametric maps of NODDI (V_{ic}, ODI, and V_{iso}), DTI (FA and MD), and DKI (MK) were generated from each subject. Representative parametric maps for typical subjects in different periods are illustrated in Fig. 2. It was shown that ischemic areas had apparent heterogeneous and high signal on the ODI and V_{ic} maps and hypointensity on the V_{iso} map. MK showed heterogeneous hyperintensity; FA and MD showed hypointensity in lesions.

3.1. Comparison of NODDI metrics between lesions and contralateral tissues

NODDI metrics in lesions were significantly different from those in contralateral normal tissues. Specific quantitative analysis of NODDI metrics between the lesions and the contralateral regions are shown in Table 1. The values of V_{ic} and ODI in lesion areas increased significantly ($P < 0.05$, respectively), whereas the V_{iso} value decreased significantly compared with contralateral regions ($P < 0.05$).

Table 1
Comparison of NODDI metrics between the lesions (L) and the contralateral tissues (C) and the absolute percentage changes between NODDI and DTI/DKI metrics.

	Hyperacute/acute/subacute		
	L	C	Percent change
V_{ic}	0.869 ± 0.062	0.545 ± 0.076	0.616 ± 0.187[a,b]
ODI	0.561 ± 0.097	0.286 ± 0.065	1.024 ± 0.415[a,b,c]
V_{iso}	0.030 ± 0.017	0.092 ± 0.037	−0.659 ± 0.154[a,b]
MK	1.393 ± 0.245	0.869 ± 0.111	0.606 ± 0.223[c]
FA	0.253 ± 0.081	0.361 ± 0.082	−0.294 ± 0.164[b]
MD	0.578 ± 0.067	0.950 ± 0.091	−0.390 ± 0.068[b]

$P < 0.05$ was considered statistically significant.
[a] Significant difference between the NODDI metrics in L and C.
[b] Significant difference between the absolute percentage changes of NODDI and DTI metrics (FA, MD versus V_{ic}, ODI, V_{iso}).
[c] Significant difference between the absolute percentage changes of ODI and MK.

3.2. Comparison of NODDI/rNOODI metrics among different stroke periods

A significant intergroup difference was found for the ODI value. From the hyperacute to subacute periods, the ODI value increased and reached the peak at the subacute period (0.426 ± 0.076, 0.544 ± 0.099, and 0.590 ± 0.080; $P < 0.05$). There were no significant intergroup differences for V_{ic} or V_{iso} values ($P = 0.860$ and $P = 0.620$, respectively; Table 2 and Fig. 3a). The rNODDI metrics had similar results, as shown in Table 3 and Fig. 3b.

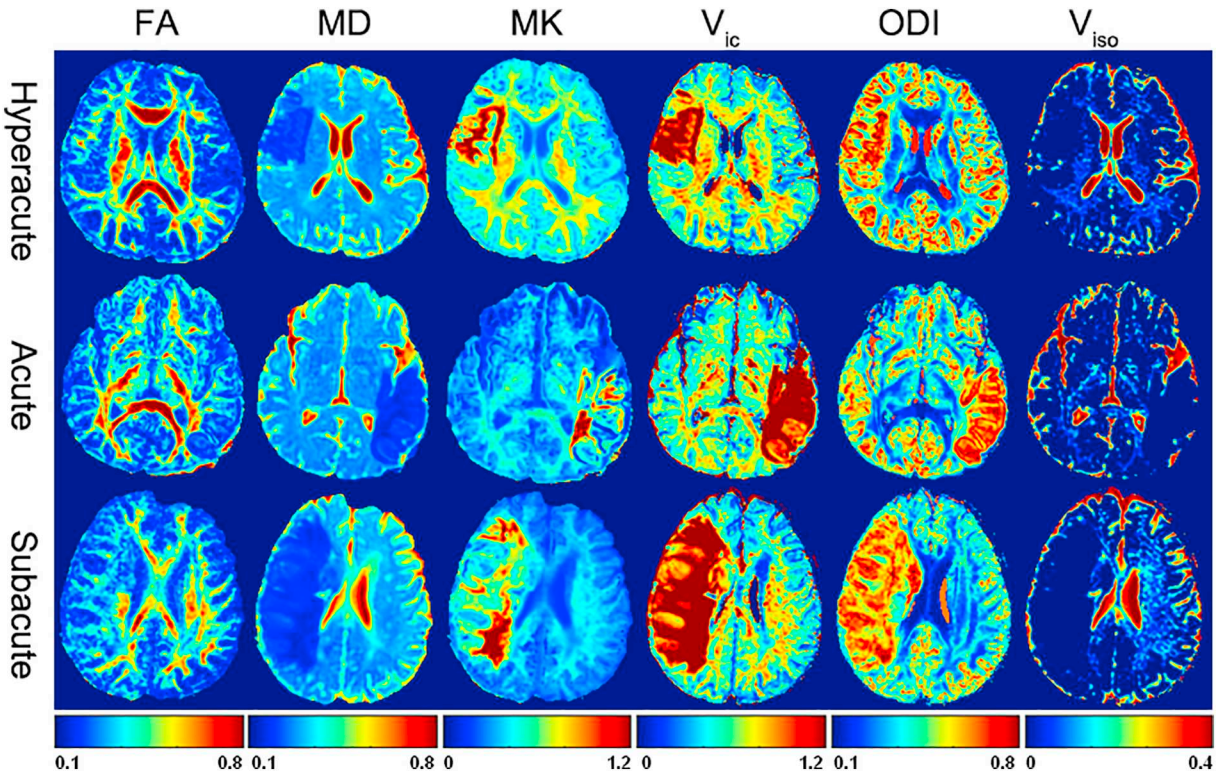

Fig. 2. FA, MD, MK, V_{ic}, ODI, and V_{iso} maps in different periods with three representative patients. Increased V_{ic}, ODI, and MK values were found, while decreased V_{iso}, FA, and MD values were observed during the hyperacute, acute, and subacute periods.

Table 2
Comparison of NODDI metrics among the hyperacute, acute, and subacute periods.

	Hyperacute	Acute	Subacute	*P*-value
V_{ic}	0.855 ± 0.073	0.869 ± 0.062	0.870 ± 0.062	0.860
ODI	0.426 ± 0.076	0.544 ± 0.099	0.590 ± 0.080	< 0.001
V_{iso}	0.028 ± 0.011	0.027 ± 0.019	0.032 ± 0.017	0.620

$P < 0.05$ was considered statistically significant.

Table 3
Comparison of rNODDI metrics among the hyperacute, acute, and subacute periods.

	Hyperacute	Acute	Subacute	*P*-value
rV_{ic}	1.557 ± 0.148	1.636 ± 0.184	1.614 ± 0.196	0.658
rODI	1.398 ± 0.214	1.885 ± 0.363	2.190 ± 0.349	< 0.001
rV_{iso}	0.350 ± 0.134	0.339 ± 0.155	0.342 ± 0.160	0.987

$P < 0.05$ was considered statistically significant.

3.3. Correlation between NODDI/rNODDI metrics and the duration since stroke onset

The value of ODI showed a fair to good positive correlation with the duration since stroke onset ($R = 0.450$, $P < 0.05$), whereas the V_{ic} and V_{iso} value showed no significant correlation with the time since stroke onset ($R = 0.089$, $P = 0.462$; $R = 0.163$, $P = 0.175$). The rNODDI metrics showed consistent results (Fig. 4).

3.4. Comparison of sensitivity between NODDI and DTI/DKI

As shown in Table 1 and Fig. 3c, in 71 patients with hyperacute/acute/subacute ischemic stroke, NODDI metrics (V_{ic}, ODI, and V_{iso}) had significantly increased absolute percentage changes compared with FA and MD metrics ($P < 0.05$, respectively), and the percentage change of ODI was significantly larger than MK ($P < 0.05$).

4. Discussion

In the present study, we demonstrated that the use of NODDI is feasible for the evaluation ischemic stroke. The ODI value showed a significant difference between hyperacute, acute, and subacute periods and had a fair to good positive correlation with the duration since stroke onset. Compared with DTI and DKI metrics, NODDI exhibited increased sensitivity in describing brain tissue microstructural changes and in investigating ischemic stroke.

NODDI is a three-compartment diffusion model with multishell and high angular resolution, which can divide the water diffusion processes in brain tissues into three diffusion pools: intracellular, extracellular, and compartments with Gaussian isotropic diffusion such as CSF [10]. The NODDI metrics include V_{ic}, which describes the density of the axons and dendrites; ODI, which describes the degree of the bending and fanning of axons and dendrites that are widespread throughout the white matter (WM) and GM; and V_{iso}, which describes the CSF volume fraction [10]. This model has shown potential in assessing ischemic stroke within only two patients [11]. For the V_{ic}, ODI, and V_{iso} maps, the contrast of normal GM/WM/CSF was consistent with the contrast depicted in Zhang's study [10]. Compared with the contralateral tissues, the significantly increased V_{ic} and ODI values and reduced V_{iso} values in ischemic lesions were found. Similar results were also previously observed in a preliminary study of WM microstructure in stroke patients using NODDI [11]. V_{ic} represents intracellular volume fraction and could reflect neurite density in the NODDI model. In the early period of ischemic stroke, the disruption of cellular energy metabolism results in a net shift of water from the extracellular to the intracellular space. This phenomenon causes an increase in the intracellular water volume fraction as well as an alteration in the relative volume of these compartments. The later period of ischemic stroke is characterized by varying degrees of demyelination, cytoskeletal collapse, necrocytosis, gliosis, and cavitation with local diffusion dead zones. These microenvironment transformations result in reduced intracellular diffusivity and reduced neurite density [20–23]. However, in our study, V_{ic} surprisingly increased during the hyperacute/acute/subacute period of ischemic stroke, which conflicted with the pathological process of ischemic stroke. This suggested that when NODDI is applied to ischemic stroke, V_{ic} can no longer be interpreted as "neurite density." Rather, the increased V_{ic} may be explained by the alteration in the relative volume of these compartments and/or the presence of restrictive structures with restrictions in all directions during stroke, which was consistent with the similarly elevated ODI as well as other, as of yet unidentified microstructural changes [24,25]. This warned us that we should be very cautious when interpreting V_{ic} in ischemic stroke, as NODDI relied on strong model assumptions to infer specific microstructural properties, and these model parameters were prefixed based on values in healthy brain tissues rather than pathological tissues [26]. ODI is a parameter measuring how nonparallel axons are dispersed about a central orientation. It assumes a cylindrically symmetric Watson distribution, which could reflect the complexity of dendrites in GM and axons in WM [10]. An increased ODI in lesions in this study may reflect the real pathological changes during ischemic stroke. Because axons and dendrites swell and bead, the loss of myelin sheath and the breaking of WM fibers led to the increased complexity of neurite orientation dispersion [2,20,23]. V_{iso} represents the diffusion fraction with the isotropic Gaussian property, which was very small compared with V_{ic} and ODI values in normal brain tissues and was found to be reduced in the lesion regions. The net shift of water from the extracellular compartment after ischemia might have led to the decrease in the fraction of water with isotropic Gaussian distribution in the extracellular space, resulting in a decrease in the V_{iso} [17,20].

Specifically, we found that the ODI value can distinguish hyperacute, acute, and subacute periods, and they showed a fair to good positive correlation with the duration since stroke onset. This may

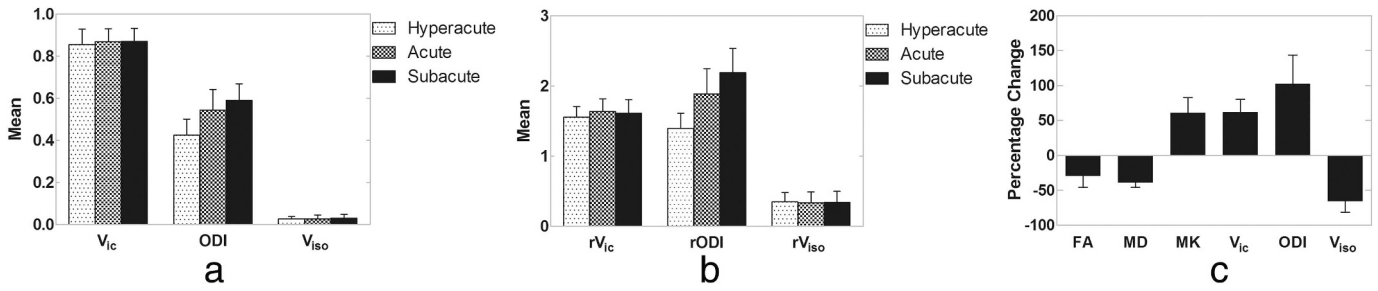

Fig. 3. Bar graphs of NODDI (a)/rNODDI (b) metrics in different periods of ischemic stroke and the percentage changes of different diffusion metrics (c). ODI/rODI value significantly increased from hyperacute to subacute, while no significant between-group differences were observed in V_{ic}/rV_{ic} and V_{iso}/rV_{iso}. Percentage changes of V_{ic}, ODI, and V_{iso} values were significant larger than MD, and percentage change of the ODI value is significant larger than MK.

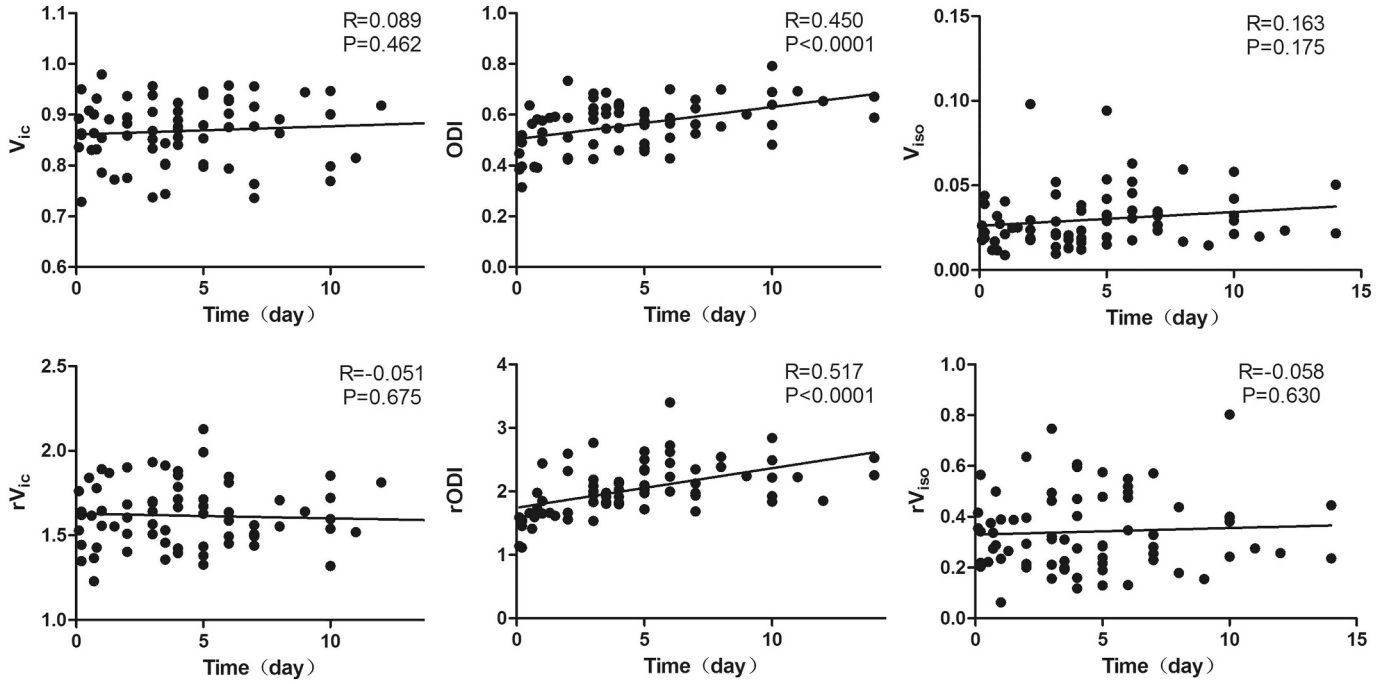

Fig. 4. Correlation between NODDI (top row)/rNODDI (bottom row) metrics and the duration since stroke onset. The values of ODI and rODI had a fair to good positive correlation with the duration since stroke onset, whereas there was no significant correlation between V_{ic}/rV_{ic} and V_{iso}/rV_{iso} values and the time since stroke onset.

indicate that the ODI value could have great potential for interpreting the underlying pathogenesis during the development process of stroke and may detect hyperacute or acute infarcted lesions, which is of great importance in the treatment of infarction [27]. In addition, the reduction in FA may be caused by the reduction in neurite density and/or the increase in the neurite orientation dispersion [10]. Our results showed increased V_{ic} and ODI; hence, the neurite orientation distribution rather than neurite density could be the key contributing factor to FA, which is in good agreement with a previous study [28].

Compared with DTI and DKI, the sensitivity of NODDI improved when investigating lesions in ischemic stroke patients. All NODDI metrics (V_{ic}, ODI, and V_{iso}) had significantly larger absolute percentage change compared with FA and MD in 71 patients, and ODI showed a significantly larger percentage change than that of MK. DKI metrics showed higher sensitivity as compared with DTI, which was also previously demonstrated by Hui using this comparison method [2].

As a novel dMRI technique, NODDI shows great potential in clinical studies. However, its inherent limitations must be acknowledged. On the one hand, NODDI relies on strong model assumptions to speculate microstructural changes, nevertheless, the assumptions of the NODDI and the interpretation of the NODDI parameters in the clinical study with different neurological disorders have been called into question [25,26,29]. Lampinen [26] demonstrated that the tortuosity assumption of NODDI enforcement of a connection between the neurite density/V_{ic} and the MD of tissue is invalid in healthy brain and glioma and that the NODDI parameter of V_{ic} should not be interpreted as being specific to neurite density. Another study regarding glioma published by Wen [25] had the similar consequence. In contrast, the studies of Grussu [30] and Sepehrband [31] showed that neurite density estimated by NODDI was in good agreement with the neurite density measured histologically in human spinal cord with multiple sclerosis and healthy mouse brain. Thus, the NODDI quantitative values of the estimated volume fractions should be carefully considered and interpreted in view of difference of brain regions and disease-specific underlying histopathological changes [32]. On the other hand, NODDI was originally developed to model normal brain tissues; however, the underlying tissue of pathology can vary in more ways, resulting in the introduction by pathological tissues of effects that are not accounted for in the model and that might not conform to the constraints of the particular model. Therefore, it may lead interpretations of the model parameters in pathology with high risk [26,33,34]. In addition, as a relatively simple compartmental model, NODDI fixes the values of several model parameters from earlier models and reduces the number of fitted parameters, which may lead to bias in the process of fitting [35]. Attention to these limitations when using the NODDI model could avoid the pitfalls of overinterpreting the resulting model parameters in pathology.

Except for the above drawbacks of NODDI, additional limitations of the study are the small sample size of the hyperacute period and the lack of longitudinal observation in the same patients. More patients may be enrolled, and a longitudinal observation of the same patients will be performed in a following study. Another limitation is that our protocol included only 25 noncollinear directions and a large slice thickness (4 mm); more directions and isotropic voxel size with a thinner slice may offer more detailed and precise information as well as avoid partial volume effects, which would be further validated in further study.

5. Conclusion

This preliminary study has demonstrated that NODDI is a potential technique for quantitatively evaluating microstructural changes in ischemic stroke patients. NODDI has a clinically feasible acquisition protocol and analysis pipeline and showed higher sensitivity when compared with DTI and DKI. The ODI parameter value was significantly different among the different periods of ischemic stroke and had a fair to good positive correlation with the duration since stroke onset, which could be regarded as a marker to estimate the evolution process and pathomechanism during ischemic stroke.

Acknowledgments

This work was supported by the National Natural Science Foundation of China (No. 81570462, 81730049, 81801666).

References

[1] Thom T, Haase N, Rosamond W, Howard VJ, Rumsfeld J, Manolio T, et al. Heart disease and stroke statistics—2006 update: a report from the American Heart Association Statistics Committee and Stroke Statistics Subcommittee. Circulation 2006;113:e85–151.

[2] Hui ES, Fieremans E, Jensen JH, Tabesh A, Feng W, Bonilha L, et al. Stroke assessment with diffusional kurtosis imaging. Stroke 2012;43:2968–73.

[3] Yoo AJ, Gonzalez RG. Clinical applications of diffusion MR imaging for acute ischemic stroke. Neuroimaging Clin N Am 2011;21:51–69.

[4] De Santis S, Gabrielli A, Palombo M, Maraviglia B, Capuani S. Non-Gaussian diffusion imaging: a brief practical review. Magn Reson Imaging 2011;29:1410–6.

[5] Ota M, Noda T, Sato N, Hidese S, Teraishi T, Setoyama S, et al. The use of diffusional kurtosis imaging and neurite orientation dispersion and density imaging of the brain in major depressive disorder. J Psychiatr Res 2018;98:22–9.

[6] Behrens TE, Woolrich MW, Jenkinson M, Johansen-Berg H, Nunes RG, Clare S, et al. Characterization and propagation of uncertainty in diffusion-weighted MR imaging. Magn Reson Med 2003;50:1077–88.

[7] Tuch DS. Q-ball imaging. Magn Reson Med 2004;52:1358–72.

[8] Wedeen VJ, Hagmann P, Tseng WY, Reese TG, Weisskoff RM. Mapping complex tissue architecture with diffusion spectrum magnetic resonance imaging. Magn Reson Med 2005;54:1377–86.

[9] Assaf Y, Freidlin RZ, Rohde GK, Basser PJ. New modeling and experimental framework to characterize hindered and restricted water diffusion in brain white matter. Magn Reson Med 2004;52:965–78.

[10] Zhang H, Schneider T, Wheeler-Kingshott CA, Alexander DC. NODDI: practical in vivo neurite orientation dispersion and density imaging of the human brain. Neuroimage 2012;61:1000–16.

[11] Adluru G, Gur Y, Anderson JS, Richards LG, Adluru N, DiBella EV. Assessment of white matter microstructure in stroke patients using NODDI. Conf Proc IEEE Eng Med Biol Soc 2014;2014:742–5.

[12] Schilling KG, Janve V, Gao Y, Stepniewska I, Landman BA, Anderson AW. Histological validation of diffusion MRI fiber orientation distributions and dispersion. Neuroimage 2018;165:200–21.

[13] By S, Xu J, Box BA, Bagnato FR, Smith SA. Application and evaluation of NODDI in the cervical spinal cord of multiple sclerosis patients. Neuroimage Clin 2017;15:333–42.

[14] Churchill NW, Caverzasi E, Graham SJ, Hutchison MG, Schweizer TA. White matter microstructure in athletes with a history of concussion: comparing diffusion tensor imaging (DTI) and neurite orientation dispersion and density imaging (NODDI). Hum Brain Mapp 2017;38:4201–11.

[15] Genc S, Malpas CB, Holland SK, Beare R, Silk TJ. Neurite density index is sensitive to age related differences in the developing brain. Neuroimage 2017;148:373–80.

[16] Grussu F, Schneider T, Zhang H, Alexander DC, Wheeler-Kingshott CA. Neurite orientation dispersion and density imaging of the healthy cervical spinal cord in vivo. Neuroimage 2015;111:590–601.

[17] Song YK, Li XB, Huang XL, Zhao J, Zhou XX, Wang YL, et al. A study of neurite orientation dispersion and density imaging in wilson's disease. J Magn Reson Imaging 2018;48:423–30.

[18] Zhang S, Zhu W, Zhang Y, Yao Y, Shi J, Wang CY, et al. Diffusional kurtosis imaging in evaluating the secondary change of corticospinal tract after unilateral cerebral infarction. Am J Transl Res 2017;9:1426–34.

[19] Yushkevich PA, Piven J, Hazlett HC, Smith RG, Ho S, Gee JC, et al. User-guided 3D active contour segmentation of anatomical structures: significantly improved efficiency and reliability. Neuroimage 2006;31:1116–28.

[20] Fung SH, Roccatagliata L, Gonzalez RG, Schaefer PW. MR diffusion imaging in ischemic stroke. Neuroimaging Clin N Am 2011;21:345–77.

[21] Goodman JA, Kroenke CD, Bretthorst GL, Ackerman JJ, Neil JJ. Sodium ion apparent diffusion coefficient in living rat brain. Magn Reson Med 2005;53:1040–5.

[22] Jiang Q, Zhang ZG, Chopp M. MRI of stroke recovery. Stroke 2010;41:410–4.

[23] Murphy TH, Li P, Betts K, Liu R. Two-photon imaging of stroke onset in vivo reveals that NMDA-receptor independent ischemic depolarization is the major cause of rapid reversible damage to dendrites and spines. J Neurosci 2008;28:1756–72.

[24] Weber RA, Hui ES, Jensen JH, Nie X, Falangola MF, Helpern JA, et al. Diffusional kurtosis and diffusion tensor imaging reveal different time-sensitive stroke-induced microstructural changes. Stroke 2015;46:545–50.

[25] Wen Q, Kelley DA, Banerjee S, Lupo JM, Chang SM, Xu D, et al. Clinically feasible NODDI characterization of glioma using multiband EPI at 7 T. Neuroimage Clin 2015;9:291–9.

[26] Lampinen B, Szczepankiewicz F, Martensson J, van Westen D, Sundgren PC, Nilsson M. Neurite density imaging versus imaging of microscopic anisotropy in diffusion MRI: a model comparison using spherical tensor encoding. Neuroimage 2017;147:517–31.

[27] Zhang S, Yao Y, Shi J, Tang X, Zhao L, Zhu W. The temporal evolution of diffusional kurtosis imaging in an experimental middle cerebral artery occlusion (MCAO) model. Magn Reson Imaging 2016;34:889–95.

[28] Jespersen SN, Leigland LA, Cornea A, Kroenke CD. Determination of axonal and dendritic orientation distributions within the developing cerebral cortex by diffusion tensor imaging. IEEE Trans Med Imaging 2012;31:16–32.

[29] Jelescu IO, Veraart J, Fieremans E, Novikov DS. Degeneracy in model parameter estimation for multi-compartmental diffusion in neuronal tissue. NMR Biomed 2016;29:33–47.

[30] Grussu F, Schneider T, Tur C, Yates RL, Tachrount M, Ianus A, et al. Neurite dispersion: a new marker of multiple sclerosis spinal cord pathology? Ann Clin Transl Neurol 2017;4:663–79.

[31] Sepehrband F, Clark KA, Ullmann JF, Kurniawan ND, Leanage G, Reutens DC, et al. Brain tissue compartment density estimated using diffusion-weighted MRI yields tissue parameters consistent with histology. Hum Brain Mapp 2015;36:3687–702.

[32] Caverzasi E, Papinutto N, Castellano A, Zhu AH, Scifo P, Riva M, et al. Neurite orientation dispersion and density imaging color maps to characterize brain diffusion in neurologic disorders. J Neuroimaging 2016;26:494–8.

[33] Lampinen B, Szczepankiewicz F, van Westen D, Englund E, C SP, Latt J, et al. Optimal experimental design for filter exchange imaging: apparent exchange rate measurements in the healthy brain and in intracranial tumors. Magn Reson Med 2017;77:1104–14.

[34] Sato K, Kerever A, Kamagata K, Tsuruta K, Irie R, Tagawa K, et al. Understanding microstructure of the brain by comparison of neurite orientation dispersion and density imaging (NODDI) with transparent mouse brain. Acta Radiol Open 2017;6:1743151992.

[35] Edwards LJ, Pine KJ, Ellerbrock I, Weiskopf N, Mohammadi S. NODDI-DTI: estimating neurite orientation and dispersion parameters from a diffusion tensor in healthy white matter. Front Neurosci 2017;11:720.